International Journal of Architectural, Civil and Construction Sciences
ISSN: 2415-1734
Vol:7, No:10, 2013

Stabilization of Steel Beams of Monosymmetric Thin-Walled Cross-Section by Trapezoidal Sheeting

Ivan Balázs, Jindřich Melcher

***Abstract*—**Steel thin-walled beams have been widely used in civil engineering as purlins, ceiling beams or wall substructure beams. There are often planar members such as trapezoidal sheeting or sandwich panels used as roof or wall cladding fastened to the steel beams. The planar members also serve as stabilization of thin-walled beams against buckling due to loss of stability. This paper focuses on problem of stabilization of steel monosymmetric thin-walled beams by trapezoidal sheeting. Some factors having influence on overall behavior of this structural system are investigated using numerical analysis. Thin-walled beams in bending stabilized by trapezoidal sheeting are of primarily interest of this study.

***Keywords*—**Beam, buckling, numerical analysis, stability, steel structures, trapezoidal sheeting.

I. Introduction

STEEL thin-walled beams are prone to losses of stability due to slenderness of the cross-section. Planar member such as trapezoidal sheeting fastened to a thin-walled beam has positive influence on resistance of the beam against flexural, torsional or lateral-torsional buckling since it increases critical force or critical moment. It is a problem of bound deformation of the beam along the span (prescribed axis of rotation) [1]. Further, structural system consisting of thin-walled steel beams in bending and trapezoidal sheeting will be treated here. The lateral buckling of the beam is prevented due to certain shear stiffness of the sheeting [2].

Actual behavior of the structural system is very complex and mathematical solution in a close form is not possible. There is number of factors affecting stabilizing performance of trapezoidal sheeting such as stiffness of planar member, way of load transfer from the sheeting to the beam, characteristics of fasteners etc. [3]. Regarding current standards for design of steel structures [4], there are some simplified provisions for stabilization of beams by trapezoidal sheeting. Some factors are taken into account by empirical coefficients. A brief outline and results of a parametric study concerning standard provisions were published in [5].

II. Subject of the Study and Assumptions

The goal of this study is to investigate stabilizing effect of selected types of trapezoidal sheeting on steel thin-walled beam in bending. A relevant problem of stability (lateral-torsional buckling) is hence dealt with. A simple beam is considered, the spans L are equal to 3m and 6m. The trapezoidal sheeting is fastened at the top flange of the beam. The sheeting is in the so called normal position. Two cases will be investigated: the ribs of sheeting are oriented in the perpendicular direction to the beam (case A) and in parallel way (case B). In both cases, the sheeting is supported on all four edges. Two types of trapezoidal sheeting from Arcelor Mittal ironworks sortiment with different depth are utilized [6]: Arval 200/420 (the depth H is 200mm) and Arval 50/262.5 (the depth H is 48mm). Various value of trapezoidal sheeting shear stiffness is thus examined. The dimensions of sheeting used can be seen in Fig. 1. The thickness of the sheeting t is 1mm. The material is steel of S320 grade (according to the producer).

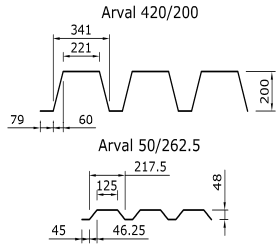

Fig. 1 Dimensions of trapezoidal sheeting

The sheeting is supported by steel thin-walled beams of monosymmetric cross-section. The hot-rolled UPE 100 and UPE 300 sections are utilized (Fig. 2).

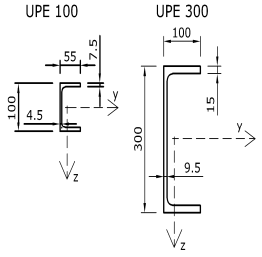

Fig. 2 Dimensions of the beams

The material is steel of the S235 grade. Fig. 2 shows also orientation of the coordinate system. The x axis is longitudinal axis of the beam.

In Fig. 3, there is a schematic picture of entire structural system.

Ivan Balázs is with the Brno University of Technology, Faculty of Civil Engineering, Institute of Metal and Timber Structures, Veveří 331/95, 602 00 Brno, Czech republic (e-mail: balazs.i@ fce.vutbr.cz).

Jindřich Melcher is with the Brno University of Technology, Faculty of Civil Engineering, Institute of Metal and Timber Structures, Veveří 331/95, 602 00 Brno, Czech republic (e-mail: melcher.j@ fce.vutbr.cz).

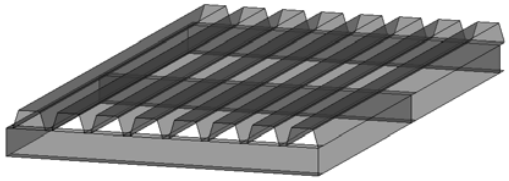

Fig. 3 Structural system

The spacing between each beam is equal to 3m. In the static point of view, trapezoidal sheeting is actually a continuous beam with two fields. The beam constituting its intermediate support will be investigated in the following parts of the paper. Its load width is 3m. The sheeting is fastened to the beam in each rib.

The load is assumed as uplift uniformly distributed load q (kN/m^2) acting on the trapezoidal sheeting. The uplift load is normally caused by wind. Under this condition, the bottom (free) flange is in compression and thereby more likely to buckle laterally.

III. Numerical Modeling

A. In General

The analysis is performed using numerical modeling. The Dlubal RFEM 4 code based on finite element method (FEM) is utilized. The structure is modeled using shell elements, finite elements network is generated automatically by the code. The thickness of each part of beams is assigned according to Fig. 2. The finite element size is set to 30mm. There is a contact between the beam and the sheeting with complete transfer of forces.

B. Supports

A special attention has to be paid to the beam supports. Since the beam is in bending, lateral-torsional buckling might occur. According to the background document [7] to the current standard for design of steel structures [8], standard fork condition should be considered when dealing with lateral-torsional buckling. It prevents lateral displacement of the beam in the supports while warping can develop freely. Standard fork support condition is schematically illustrated in Fig. 4.

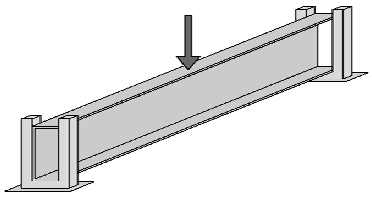

Fig. 4 Fork support condition

The implementation of fork conditions in the finite element model can be seen in Fig. 5. In practice, the fork support conditions can be affected by stiffeners at the supports [9].

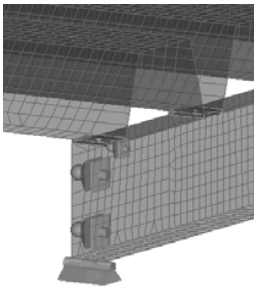

Fig. 5 Implementation of fork support conditions

The sheeting is supported at all four edges. The support of its edge perpendicular to the investigated sheeting is modeled in a simplified way using flexible support with stiffness corresponding to stiffness of the section UPE 100 or UPE 300, respectively.

C. Imperfections

Since stability of thin-walled steel members is investigated, proper implementation of imperfections is of big importance. The imperfections take into account behavior of real thin-walled member. It is possible to implement them in the form of initial curvature, see Fig. 6. Its amplitude for thin-walled slender beams e_0 is given in the standard [8] according to appropriate lateral-torsional buckling curve.

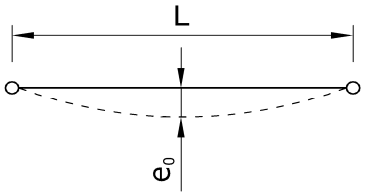

Fig. 6 Initial imperfection of the beam

For hot-rolled U-section, a curve d applies. The amplitude of initial curvature e_0 for this instance for flexural buckling is given by (1), where L is span of the beam.

$$e_0 = \frac{L}{150} \tag{1}$$

When dealing with lateral-torsional buckling, it is possible to consider it as half of the given value [8] so that (2) applies:

$$e_0 = \frac{L}{300} \tag{2}$$

In the considered cases (span of the beam L is 3m or 6m), the amplitudes of initial curvature of the beam are 10mm or 20mm).

In case of trapezoidal sheeting, the phenomenon of local buckling might occur. Its character differs somewhat from the phenomenon of overall buckling of beams. The appropriate amplitude of initial imperfection for local buckling of compressed flange should be implemented carefully.

According to [10], the amplitude of initial buckling Δ (mm) can be given as in (3), where t (mm) is the thickness of sheeting.

$$\Delta = 6 \cdot t \cdot \exp(-2 \cdot t) \quad (3)$$

In this case (thickness of the sheeting t is 1mm) the amplitude of initial buckling calculated according to equation (3) is 0.81mm, see Fig. 7.

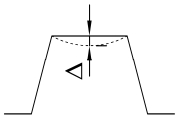

Fig. 7 Initial imperfection of the sheeting

D. Process of the Numerical Analysis

Within the frame of the numerical modeling, stability analysis using RF-STABILITY module of the RFEM code was performed. The first eigenmode was adopted as the mode of initial buckling (curvature) with given amplitudes. The geometry of the beam and sheeting was modified according to the first eigenmode using RF-IMP module of the RFEM code so that "real" (imperfect) members were thereby obtained. This module enables to update geometry of a structural system according to desired eigenmode gained from preceding stability analysis. After this, a geometrically nonlinear analysis (2nd order theory) of the imperfect system (GNIA analysis) is ready to be performed [11]. In the following figures (Figs. 8 and 9), the initial imperfections created by the RFEM code can be seen. For the reason of better clarity, there is the imperfection of part of the sheeting only in Fig. 9.

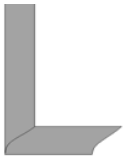

Fig. 8 Initial imperfection of the beam (bottom flange, from below)

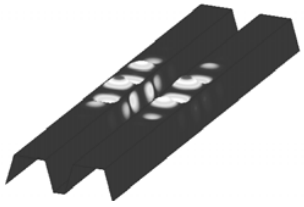

Fig. 9 Initial imperfection of the sheeting (detail)

Having defined the geometry of the structural system, load, support conditions, materials and implemented the initial imperfections, the geometrically nonlinear analysis can be performed. The uplift uniformly distributed load q was incrementally increased until the analysis stopped due to convergence problem. Achieved load magnitude was recorded. In all cases, this occurred because of instabilities in the trapezoidal sheeting finite element network. This corresponds to the expected mode of failure of the trapezoidal sheeting due to local buckling of extremely thin walls of the sheeting. The sheeting is thereby limiting factor in such structural systems.

The behavior of the UPE beams was investigated more detailed. The values of the internal forces in the preceding step before collapse were recorded and evaluated. Since shell elements were utilized in the FEM analysis, specific internal forces n (kN/m) were obtained and appropriate value of stress were calculated manually using (4), where σ is normal stress and t is thickness of appropriate part of the beam (top flange, bottom flange, web). Regarding the beam, other internal forces than n_x were of low magnitude and therefore neglected.

$$\sigma = \frac{n}{t} \quad (4)$$

The magnitude of displacement u (mm) was recorded as well. Since the beam is considered and modeled as simple beam, the magnitudes of internal forces and displacements were read at nodes of finite element network at midspan of the beam.

The calculated magnitudes of the normal stress $\sigma_x$will be used for the check of the beam load-carrying capacity using (5), where f_y(MPa) is yield strength of the material of the beam (235MPa for S235 steel). If (5) is fulfilled, the check is satisfactory.

$$\sigma_x \leq f_y \quad (5)$$

IV. Results of the Numerical Analysis

The results of geometrically nonlinear numerical analyses of imperfect structures are divided into two groups: case A (ribs of sheeting in the perpendicular direction to the beam) and case B (ribs in the longitudinal direction). Both cases are further divided according to the type of the beam (UPE 100, UPE 300) and according to the depth H of the trapezoidal sheeting.

A. Case A – Perpendicular Orientation of the Ribs

The situation is drawn in Fig. 10.

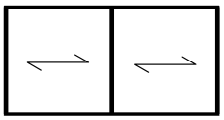

Fig. 10 Case A

In Table I there are maximum magnitudes of uniformly distributed uplift load q (kN/m^2) and appropriate deflection u (mm) of the simple beam read at midspan.

TABLE I
PARTIAL RESULTS

Span L (m)	Beam cross-section	Depth of the sheeting H (mm)	Maximum magnitude of the load q (kN/m^2)	Deflection at midspan u (mm)
3	UPE 100	48	0.65	5.44
3	UPE 100	200	0.82	10.37
3	UPE 300	48	1.75	0.82
3	UPE 300	200	2.20	1.41
6	UPE 100	48	1.47	156.96
6	UPE 100	200	0.31	25.20
6	UPE 300	48	1.97	7.37
6	UPE 300	200	0.40	1.32

The magnitudes of specific normal force n_x (kN/m) were read in the four significant nodes of the UPE section, where the flange of the section turns into the web. These nodes are plotted in Fig. 11. The appropriate magnitudes of normal stress σ_x were calculated using (4). The flange thickness of the UPE 100 section is 7.5mm and of the UPE 300 section 15.0mm.

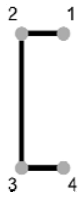

Fig. 11 Significant nodes to read the results

In the following tables there are magnitudes of internal force n_x(kN/m) obtained from the RFEM code in the above-mentioned nodes as well as appropriate magnitudes of normal stress σ_x(MPa). Tables II and III apply for the UPE 100 section.

TABLE II
INTERNAL FORCES AND STRESSES, UPE 100 SECTION, L = 3 M

Sheeting Type	Node	Specific normal force n_x (kN/m)	Normal stress σ_x(MPa)
Arval 50/262.5	1	325.2	43.4
Arval 50/262.5	2	307.5	41.0
Arval 50/262.5	3	-384.8	-51.3
Arval 50/262.5	4	-338.6	-45.1
Arval 420/200	1	549.6	73.3
Arval 420/200	2	505.3	67.4
Arval 420/200	3	-534.0	-71.2
Arval 420/200	4	-485.8	-64.8

TABLE III
INTERNAL FORCES AND STRESSES, UPE 100 SECTION, L = 6 M

Sheeting Type	Node	Specific normal force n_x (kN/m)	Normal stress σ_x(MPa)
Arval 50/262.5	1	2555.6	340.7
Arval 50/262.5	2	2741.8	365.6
Arval 50/262.5	3	-2737.8	-365.0
Arval 50/262.5	4	-3024.0	-403.2
Arval 420/200	1	510.4	68.1
Arval 420/200	2	454.9	60.7
Arval 420/200	3	-481.1	-64.1
Arval 420/200	4	-430.6	-57.4

In Figs. 12 and 13, there are normal stress diagrams corresponding to the results listed in Tables II and III, respectively.

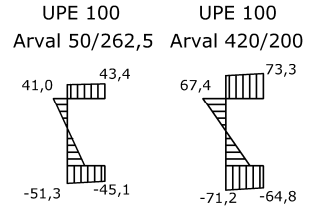

Fig. 12 Normal stress diagrams (L = 3 m)

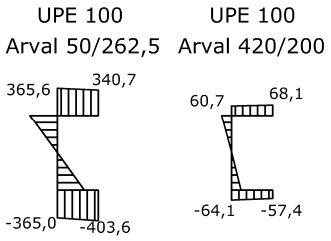

Fig. 13 Normal stress diagrams (L = 6 m)

There is analogical data for the UPE 300 section in Tables IV and V.

TABLE IV
INTERNAL FORCES AND STRESSES, UPE 300 SECTION, L = 3 M

Sheeting Type	Node	Specific normal force n_x (kN/m)	Normal stress σ_x(MPa)
Arval 50/262.5	1	146.1	9.7
Arval 50/262.5	2	137.3	9.2
Arval 50/262.5	3	9.1	0.6
Arval 50/262.5	4	-213.7	-14.2
Arval 420/200	1	318.7	21.2
Arval 420/200	2	308.8	20.6
Arval 420/200	3	-353.3	-23.6
Arval 420/200	4	-202.4	-13.5

TABLE V
INTERNAL FORCES AND STRESSES, UPE 300 SECTION, L = 6 M

Sheeting Type	Node	Specific normal force n_x (kN/m)	Normal stress σ_x(MPa)
Arval 50/262.5	1	736.1	49.1
Arval 50/262.5	2	745.4	49.7
Arval 50/262.5	3	-731.3	-48.8
Arval 50/262.5	4	-778.4	-51.9
Arval 420/200	1	141.1	9.4
Arval 420/200	2	144.9	9.7
Arval 420/200	3	-145.4	-9.7
Arval 420/200	4	-138.9	-9.3

In Figs. 14 and 15, there are normal stress diagrams corresponding to the results listed in Tables IV and V, respectively.

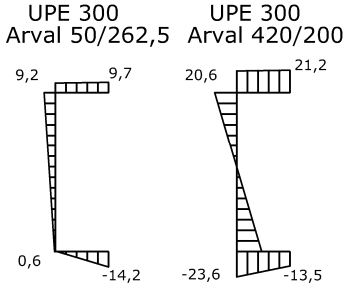

Fig. 14 Normal stress diagrams (L = 3 m)

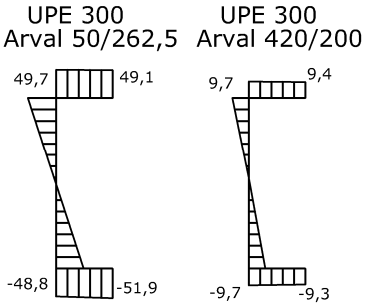

Fig. 15 Normal stress diagrams (L = 6 m)

B. Case B – Longitudinal Orientation of the Ribs

In the following tables and figures there are analogical results for the case B. In Fig. 16 there is the situation of the Case B.

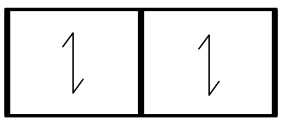

Fig. 16 Case B

In Table VI, there are maximum achieved magnitudes of uplift load q (kN/m2) and appropriate deflections at midspan of the simple beam.

TABLE VI
PARTIAL RESULTS

Span L (m)	Beam cross-section	Depth of the sheeting H (mm)	Maximum magnitude of the load q (kN/m^2)	Deflection at midspan u (mm)
3	UPE 100	48	3.60	5.28
3	UPE 100	200	4.10	10.70
3	UPE 300	48	4.05	0.53
3	UPE 300	200	4.75	0.93
6	UPE 100	48	0.70	9.80
6	UPE 100	200	1.80	8.63
6	UPE 300	48	0.72	1.29
6	UPE 300	200	1.90	1.17

The internal forces and appropriate normal stresses at significant nodes of the beam are listed in Tables VII and VIII for the UPE 100 section and in Tables IX and X for the UPE 300 section according to the trapezoidal sheeting type used.

TABLE VII
INTERNAL FORCES AND STRESSES, UPE 100 SECTION, L = 3 M

Sheeting Type	Node	Specific normal force n_x (kN/m)	Normal stress σ_x(MPa)
Arval 50/262.5	1	125.3	16.7
Arval 50/262.5	2	174.5	23.3
Arval 50/262.5	3	-354.2	-47.2
Arval 50/262.5	4	-175.2	-23.4
Arval 420/200	1	72.5	9.7
Arval 420/200	2	94.6	12.6
Arval 420/200	3	-422.7	-56.4
Arval 420/200	4	199.8	26.6

TABLE VIII
INTERNAL FORCES AND STRESSES, UPE 100 SECTION, L = 6 M

Sheeting Type	Node	Specific normal force n_x (kN/m)	Normal stress σ_x(MPa)
Arval 50/262.5	1	129.3	17.2
Arval 50/262.5	2	108.5	14.5
Arval 50/262.5	3	-218.7	-29.2
Arval 50/262.5	4	-190.0	-25.3
Arval 420/200	1	16.4	2.2
Arval 420/200	2	59.8	8.0
Arval 420/200	3	-186.3	-24.8
Arval 420/200	4	-265.8	-35.4

TABLE IX
INTERNAL FORCES AND STRESSES, UPE 300 SECTION, L = 3 M

Sheeting Type	Node	Specific normal force n_x (kN/m)	Normal stress σ_x(MPa)
Arval 50/262.5	1	51.2	3.4
Arval 50/262.5	2	102.6	6.8
Arval 50/262.5	3	-118.0	-7.9
Arval 50/262.5	4	26.6	1.8
Arval 420/200	1	-11.4	-0.8
Arval 420/200	2	109.4	7.3
Arval 420/200	3	-142.5	-9.5
Arval 420/200	4	70.7	4.7

TABLE X
INTERNAL FORCES AND STRESSES, UPE 300 SECTION, L = 6 M

Sheeting Type	Node	Specific normal force n_x (kN/m)	Normal stress σ_x(MPa)
Arval 50/262.5	1	103.4	6.9
Arval 50/262.5	2	100.2	6.7
Arval 50/262.5	3	-85.0	-5.7
Arval 50/262.5	4	-9.2	-0.6
Arval 420/200	1	7.9	0.5
Arval 420/200	2	81.6	5.4
Arval 420/200	3	-85.3	-5.7
Arval 420/200	4	-64.0	-4.3

The corresponding diagrams of normal stress are in Figs. 17, 18 (UPE 100 section) and Figs. 19, 20 (UPE 300 section).

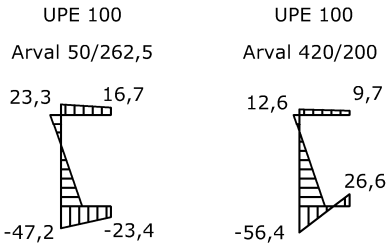

Fig. 17 Normal stress diagrams (L = 3m)

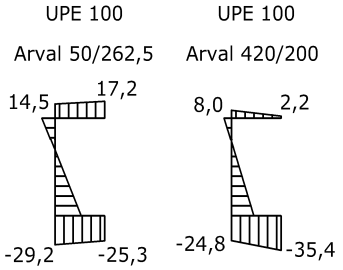

Fig. 18 Normal stress diagrams (L = 6 m)

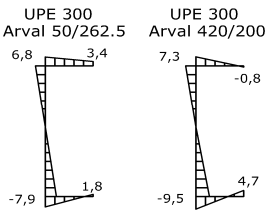

Fig. 19 Normal stress diagrams (L = 3 m)

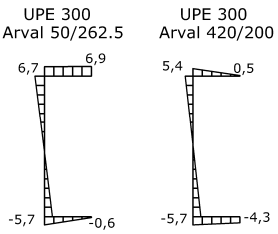

Fig. 20 Normal stress diagrams (L = 6 m)

C. Graphical Outputs of the Numerical Analysis

Selected representative graphical outputs obtained from the RFEM code are displayed in the following figures. In Figs. 21 and 22 there are images of deformation. The normal force n_x diagram is displayed in Fig. 23.

Fig. 21 Deformation (UPE 300 and Arval 420/200, L = 3 m)

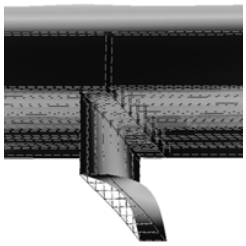

Fig. 22 Deformation (UPE 300 and Arval 420/200, L = 3 m)

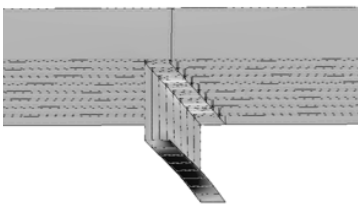

Fig. 23 Normal force n_x (UPE 300 and Arval 420/200, L = 3 m)

D. Comparison with Beams with No Stabilization

For the purpose of comparison, numerical analyses of UPE 100 and UPE 300 sections with no stabilization were performed. All the rest of assumptions listed above remained unaltered as well as the procedure of the analysis. Unlike the above mentioned structural systems where areal uniformly distributed uplift load q (kN/m^2) applied on the sheeting was considered, now only linear uniformly distributed load $q_{lin.}$ (kN/m) intersecting the center of gravity acting on the top flange of the section was applied. The comparison is presented in Table XI and Fig. 24 for the UPE 100 section and in Table XII and Fig. 25 for the UPE 300 section, both for the span L = 3m. There are also magnitudes of deflections at midspan. For the beams stabilized by trapezoidal sheeting, the maximum magnitude of loading is the loading when the analysis failed due to instabilities in the trapezoidal sheeting finite element network. For the beams with no stabilization, the magnitude of the load is the load that causes stress equal to yield strength at midspan in the beam. Areal loads were modified to linear loads using load width. In Table XIII and Fig. 26 and Table XIV and Fig. 27 there are analogical results for the span L = 6m.

TABLE XI
COMPARISON, UPE 100 SECTION, L = 3 M

Stabilization	Areal load q (kN/m^2)	Linear load q_{lin}(kN/m)	Deflection u (mm)
No stabilization	-	6.20	35.62
Case A, H = 48 mm	0.65	1.95	5.44
Case A, H = 200 mm	0.82	2.46	10.37
Case B, H = 48 mm	3.60	10.80	5.28
Case B, H = 200 mm	4.10	12.30	10.70

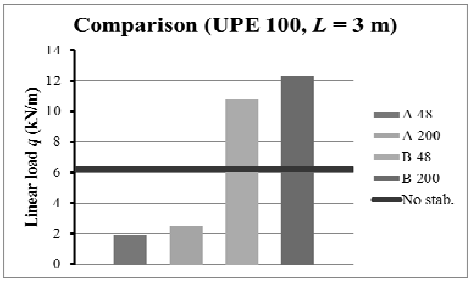

Fig. 24 Graphical representation of results acc. to Table XI

TABLE XII
COMPARISON, UPE 300 SECTION, L = 3 M

Stabilization	Areal load q (kN/m^2)	Linear load q_{lin}(kN/m)	Deflection u (mm)
No stabilization	-	67.50	21.59
Case A, H = 48 mm	1.75	5.25	0.82
Case A, H = 200 mm	2.20	6.60	1.41
Case B, H = 48 mm	4.05	12.15	0.53
Case B, H = 200 mm	4.75	14.25	0.93

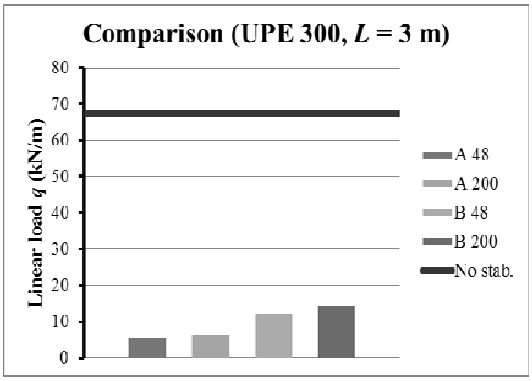

Fig. 25 Graphical representation of results acc. to Table XII

TABLE XIII
COMPARISON, UPE 100 SECTION, L = 6 M

Stabilization	Areal load q (kN/m^2)	Linear load q_{lin}(kN/m)	Deflection u (mm)
No stabilization	-	1.40	100.86
Case A, H = 48 mm	1.47	4.41	156.96
Case A, H = 200 mm	0.31	0.93	25.20
Case B, H = 48 mm	0.70	2.10	9.80
Case B, H = 200 mm	1.80	5.40	8.63

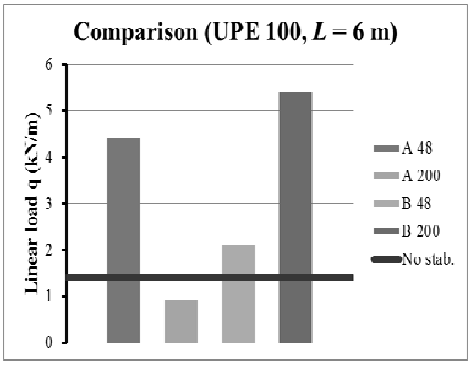

Fig. 26 Graphical representation of results acc. to Table XIII

TABLE XIV
COMPARISON, UPE 300 SECTION, L = 6 M

Stabilization	Areal load q (kN/m^2)	Linear load q_{lin}(kN/m)	Deflection u (mm)
No stabilization	-	17.3	59.78
Case A, H = 48 mm	1.97	5.91	7.37
Case A, H = 200 mm	0.40	1.20	1.32
Case B, H = 48 mm	0.72	2.16	1.29
Case B, H = 200 mm	1.90	5.70	1.17

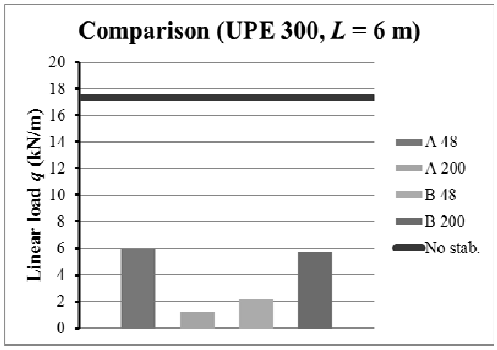

Fig. 27 Graphical representation of results acc. to Table XIV

For more detailed results of comprehensive numerical analyses of steel beams of monosymmetric thin-walled cross-sections in bending and torsion, the reader is referred e.g. to [12].

V. SUGGESTIONS FOR FURTHER RESEARCH

There are several possibilities to develop the presented problem. Regarding numerical modeling, it is possible to utilize finite elements of smaller dimension to get more precise results or to utilize spatial elements instead of the shell ones. The latter option is however associated with demanding requirements for performance of computer used for analyses and requires significantly longer computing time. Parametric study dealing with influence of the size of the finite elements on accuracy of the results can be performed. Another way to proceed might be more accurate modeling of the beam-sheeting connection, especially in the point of view of stiffness or flexibility of fasteners. The influence of some factors having influence on the stabilization of beams can be assisted by testing.

VI. Conclusion

This paper summarizes results of numerical geometrically nonlinear analyses of structures consisting of a thin-walled beam and trapezoidal sheeting fastened at the top flange of the beam. The analyses were performed using finite element method and focused on stabilization of the beam by the trapezoidal sheeting. The uplift load was applied over the entire surface of the sheeting so that the free flange of the beam was in compression and prone to the loss of stability. With the exception of one case of exceeding yield strength (see Fig. 13), all the investigated cases met the requirements for satisfactory check of normal stress including lateral-torsional buckling (5) for given span of the beam. The rate of stabilization for these cases is thereby sufficient.

The results show that trapezoidal sheeting is usually limiting factor in these structures. The failure of the sheeting occurs normally sooner than normal stress in the beam reaches the yield strength so the sheeting limits the maximum permissible load.

The presented graphical outputs display expected behavior of the monosymmetric sections used in this study. The top flange is supported by the sheeting, the bottom one is free and hence displacement can develop. Since the shear center of the U-section is situated outside of the section the load acts eccentrically. It results in torsion of the section. It is also evident from the normal stress diagrams.

The paper brings some suggestions for further research and some ideas for more precise numerical modeling.

Acknowledgment

The paper was elaborated within the support of the projects of FAST-J-13-2059, FAST-J-13-2036 and GACR No. P105/12/0314.

References

[1] V. Březina, *Buckling resistance of metal bars and beams (Vzpěrnáúnosnostkovovýchprutů a nosníků)*. Prague: Czechoslovak Academy of Sciences, 1962

[2] J. Lindner, "Beams in bending restraint by rotational spring stiffness and shear stiffness of adjacent members (ZurAussteifung von BiegeträgerndurchDrehbettung und Schubsteifigkeit)," *Stahlbau*, vol. 77, pp. 427–435, June 2008.

[3] J. Melcher, *Bending, Torsion and Stability of Steel Beams (Ohyb, kroucení a stabilitaocelovýchnosníků)*. Brno: Brno University of Technology, 1975

[4] EN 1993-1-3, *Eurocode 3: Design of Steel Structures – Part 1-3: General Rules – Supplementary Rules for Cold-Formed Members and Sheeting (Eurokód 3: Navrhováníocelovýchkonstrukcí – Část 1-3: Obecnápravidla – Doplňujícípravidla pro tenkostěnnézastudenatvarovanéprvky a plošnéprvky)*. Prague: Czech Standard Institute, 2008.

[5] I. Balázs, J. Melcher and M. Horáček, "Stabilisation of Beams by Trapezoidal Sheeting: Parametric Study," in *Proceedings of the 3rd European Conference of Civil Engineering (ECCIE '12)*, Paris, 2012, pp. 223–227.

[6] *Arval: Static Tables (Arcelor Mittal)* (Web page). http://www.arcelormittal.com/distributionsolutions/repo/AMC%20Eastern%20Europe/DOCUMENTATION/cz/Arval%20-%20Statick%C3%A9%20tabulky%20%28v%C3%BDroba%20Senica%29.pdf, 2013.

[7] G. Sedlacek and J. Naumes, *Excerpt from the Background Document to EN 1993-1-1: Flexural Buckling and Lateral Buckling on a Common Basis: Stability Assessments According to Eurocode 3*. Aachen: Institut und LehrstuhlfürStahlbau und Leichtmetallbau, Rheinisch-WestfälischetechnischeHochschule, 2004.

[8] EN 1993-1-1, *Eurocode 3: Design of Steel Structures – Part 1-1: General Rules and Rules for Buildings (Eurokód 3: Navrhováníocelovýchkonstrukcí – Část 1-1: Obecnápravidla a pravidla pro pozemnístavby)*. Prague: Czech Standard Institute, 2006.

[9] J. Lindner and T. Holberndt, "Lateral torsional buckling capacity of beams supported at the lower flange only" in *Stability and Ductility of Steel Structures (SDSS 2002)*, Budapest, 2002, pp. 47–56.

[10] A. Ježek, Trapezoidal Sheeting Acting as Multi-Span Beams (Trapézovéplechypůsobícíjakospojiténosníky), doctoral thesis, Prague, August 2009.

[11] R. Kindmann and Ch. Wolf, "Member imperfections for verifications against lateral buckling of compression members (Geometrische Ersatzimperfektionenfür Tragfähigkeitsnachweisezum Biegeknicken von Druckstäben)," *Stahlbau*, vol. 78, pp. 25–34, Jan. 2009.

[12] I. Balázs and J. Melcher, "Geometrically nonlinear analysis of steel beams of monosymmetric thin-walled cross-sections loaded perpendicularly to the axis of symmetry (Geometrickynelineárníanalýzaocelovýchtenkostěnnýchnosníkůjednoose symetrickéhoprůřezuzatíženýchkolmo k osesymetrie)," in *Modelling in mechanics 2013: Proceedings of scientific conference*, Ostrava, 2013.